Novel Pathway of SO$_2$ Oxidation in the Atmosphere: Reactions with Monoterpene Ozonolysis Intermediates and Secondary Organic Aerosol

Jianhuai Ye[1], Jonathan P. D. Abbatt[2], Arthur W.H. Chan[1]

[1]Department of Chemical Engineering & Applied Chemistry, University of Toronto, Toronto, Canada
[2]Deparment of Chemistry, University of Toronto, Toronto, Canada

Correspondence to: Arthur W.H. Chan (arthurwh.chan@utoronto.ca)

Abstract. Ozonolysis of monoterpenes is an important source of atmospheric biogenic secondary organic aerosol (BSOA). While enhanced BSOA formation has been associated with sulfate-rich conditions, the underlying mechanisms remain poorly understood. In this work, the interactions between SO$_2$ and reactive intermediates from monoterpene ozonolysis were investigated under different humidity conditions (10% vs. 50%). Chamber experiments were conducted with ozonolysis of α-pinene or limonene in the presence of SO$_2$. Limonene SOA formation was enhanced in the presence of SO$_2$, while no significant changes in SOA yields were observed during α-pinene ozonolysis. Under dry conditions, SO$_2$ primarily reacted with stabilized Criegee Intermediates (sCI) produced from ozonolysis, but at 50% RH, heterogeneous uptake of SO$_2$ onto organic aerosol was found to be the dominant sink of SO$_2$, likely owing to reactions between SO$_2$ and organic peroxides. This SO$_2$ loss mechanism to organic peroxides in SOA has not previously been identified in experimental chamber study. Organosulfates were detected and identified using electrospray ionization-ion mobility time of flight mass spectrometer (ESI-IMS-TOF) when SO$_2$ was present in the experiments. Our results demonstrate the synergistic effects between BSOA formation and SO$_2$ oxidation through sCI chemistry and SO$_2$ uptake onto organic aerosol and illustrate the importance of considering the chemistry of organic and sulfur-containing compounds holistically to properly account for their reactive sinks.

1. Introduction

Secondary organic aerosol (SOA) is formed from condensation of low-volatility products from atmospheric oxidation of volatile organic compounds (VOCs) and comprises a major fraction of atmospheric organic aerosol (Jimenez et al., 2009). Globally, the dominant fraction of SOA is formed from oxidation of biogenic precursors, as suggested by the high fractions of modern carbon in atmospheric organic aerosol (Goldstein et al., 2009; Weber et al., 2007; Szidat et al., 2006; de Gouw et al., 2005). While emissions of biogenic hydrocarbons are largely uncontrollable, laboratory studies and field observations have shown that biogenic SOA (BSOA) formation is influenced by anthropogenic emissions, such as primary organic aerosol and NO_X (Ye et al., 2016; Xu et al., 2015; Goldstein et al., 2009; Ng et al., 2007, 2008). As a result, it has been suggested that atmospheric BSOA could be significantly reduced by controlling anthropogenic pollutants (Carlton et al., 2010; Heald et al., 2008).

One important pollutant that can affect BSOA formation is SO_2, with up to 94% of its emissions from anthropogenic activities such as fuel combustion in the U.S. (Year 2014; U.S. EPA, 2014) and more than 78% globally (Year 2007-2009; McLinden et al., 2016). Oxidation of SO_2 in the atmosphere leads to formation of sulfuric acid that plays a crucial role in atmospheric new particle formation (Brock et al., 2002) and enhances SOA formation through acid-catalyzed mechanisms (Jang et al., 2002). Long-term ground observations in Southeast U.S. show that the decrease of BSOA is correlated strongly to the decrease in sulfate content in aerosols (Marais et al., 2017), implying co-benefits in controlling SO_2 emission to reduce both sulfate and BSOA. It is further demonstrated by Xu et al. (2015) that anthropogenic NO_X and sulfate correlate strongly with 43-70% of total measured organic aerosol in this area. The mechanisms by which sulfate influences BSOA formation have also been demonstrated through laboratory studies. For example, SOA yields of isoprene, as well as α-pinene and limonene, increased with increasing the acidity of the seed aerosol (Iinuma et al., 2007; Surratt et al., 2007; Gao et al., 2004; Czoschke et al., 2003). The formation of high-molecular-weight (high-MW) oligomers and organosulfates is enhanced in the presence of sulfuric acid (Surratt et al., 2008; Tolocka et al., 2004).

There is also increasing evidence that SO_2 may directly influence BSOA formation by influencing OH reactivity. In the presence of SO_2, enhanced gas-phase products from α-pinene and β-pinene photooxidation were observed with a decreased oxidation state of gas-phase semivolatile species (Friedman et al., 2016). Liu et al. (2017) demonstrated that SOA yields of cyclohexene photooxidation were lower at atmospherically relevant concentrations of SO_2, implying that SO_2 may indirectly decrease SOA formation when the acid-catalyzed SOA enhancement is insufficient to compensate for the loss of OH reactivity towards VOCs. SO_2 can also directly influence VOC oxidation mechanisms through reactions with stabilized Criegee intermediates (sCI) formed from olefin ozonolysis (Huang et al., 2015a; Welz et al., 2012). Field observations suggested that SO_2 + sCIs reactions may contribute up to 50% of the total gaseous sulfuric acid production in the forest atmosphere, which is comparable to that from gas-phase oxidation by OH (Mauldin III et al., 2012). Consistent with this observation, model calculations with CH_2OO, the simplest sCI, suggested that the SO_2 and sCI reaction could be significant in atmospheric sulfuric acid formation under dry conditions, but suggest that this pathway may become less important as humidity increases due to the scavenging effect of water and water dimer towards sCIs (Calvert and Stockwell, 1983). However, the reactivity of sCI towards SO_2 is observed to be strongly dependent on its molecular structure. While CH_2OO may primarily react with water and water dimer, Huang et al. (2015) demonstrated that the di-substituted sCI has a long lifetime under atmospherically relevant humidity conditions and may react with SO_2. Sipilä et al. (2014) also demonstrated that the formation rates of sulfuric acid, the product of the sCI + SO_2 reaction, are nearly independent of humidity for monoterpene ozonolysis. In addition to OH and sCIs, it has been proposed that SO_2 may react with peroxy radicals (RO_2) (Kan et al., 1981). While the gas-phase reaction of SO_2 + RO_2 is usually too slow to compete with other RO_2 sinks (Berndt et al., 2015), Richards-Henderson et al. (2016) proposed that in polluted areas ($[SO_2] \geq 40$ ppb), SO_2 may react with RO_2 radicals at the surface of aerosol, and significantly accelerate (10-20 times higher) the heterogeneous oxidation rate of aerosol by OH radicals through chain propagation mechanism of alkoxy radicals. The reaction rate of particle-phase SO_2 + RO_2 ($\sim 10^{-13}$ cm^3 $molecule^{-1}$ s^{-1}) was calculated to be 4 orders of magnitude larger than that for the gas phase (10^{-17} cm^3 $molecule^{-1}$ s^{-1}) (Richards-Henderson et al., 2016), indicating that this mechanism may be important for heterogeneous oxidation of aerosols, but the contribution to SO_2 sink is likely small.

80

Not only can SO_2 react with reactive species in the gas phase, it can also either partition into aqueous droplets and submicron particles or through heterogeneous reactions with the potential to alter SOA formation mechanisms and products. Reactions with dissolved H_2O_2 and O_3 are usually considered as the dominant sinks of SO_2 in aqueous droplets (Seinfeld and Pandis, 2006), and the reaction rates are a strong

85 function of particle acidity (Hung and Hoffmann, 2015; Seinfeld and Pandis, 2006). However, it was highlighted that in polluted areas, dissolved NO_2 and heterogeneous reactions on the surface of mineral dust could also contribute significantly to atmospheric SO_2 oxidation (He et al., 2014; Xue et al., 2016). More recently, Shang et al. (2016) and Passananti et al. (2016) proposed that without assistance of other oxidants, gaseous SO_2 can also be directly taken up by unsaturated fatty acid or long-chain alkenes

90 through a [2+2] cycloaddition mechanism under atmospheric conditions with observation of organic sulfur compounds as direct formation products.

Despite the importance of SO_2 in modulating BSOA formation, there have been few studies investigating the role of SO_2 in SOA formation from monoterpene ozonolysis, an important source of BSOA. In this

95 work, we study the direct interactions between SO_2 and reactive intermediates formed from ozonolysis of limonene and α-pinene, two important monoterpenes. We hypothesize that the presence of SO_2 changes SOA formation mechanisms and may lead to changes in SOA products and SOA yields. Interactions between SO_2 and reactive intermediates such as sCI and organic peroxides during SOA formation were investigated under different humidity conditions. We report synergistic effects between SOA formation

100 and SO_2 oxidation with observation of organosulfate formation. Results in this study provide a better mechanistic understanding of BSOA formation and atmospheric SO_2 oxidation.

2. Experimental Methods

Experiments were conducted both in a 1-m^3 Teflon chamber for examining the time evolution of gaseous species and particles, and in a quartz flow tube for collection of particles onto filters and offline chemical

105 analysis.

2.1 Chamber experiments

Before each experiment, the chamber was flushed with purified air until the total particle number concentration, ozone concentration and SO_2 concentration was less than 10 # cm^{-3}, 1 ppb and 1 ppb, respectively. (R)-Limonene (97%, Sigma-Aldrich)/cyclohexane (99%, Caledon Laboratories Ltd.) or α-pinene (99%, Sigma-Aldrich)/cyclohexane solution was injected into a glass vessel and then introduced into the chamber by purified compressed air at a flow rate of ~ 10 L min^{-1}. The injection ratio (v/v) of limonene/cyclohexane and α-pinene/cyclohexane was 1:1500 and 1:500, respectively. At these ratios, the reaction of OH with cyclohexane is calculated to be around 100 times faster than that of OH with monoterpene. SO_2 (5.2 ppm, balanced in N_2, Linde Canada) was injected into the chamber at 10 L min^{-1} to achieve the desired initial concentrations. Ozone was added at a concentration more than 5 times higher than that of monoterpene to ensure complete consumption. Ammonium sulfate seed particles were introduced by a collison type atomizer (TSI 3076). In dry experiments (10-16% RH), seed particles were dried using a custom-made diffusion dryer before injection into the chamber. In humid experiments, seed particles were not dried when injected into the chamber. Chamber RH was controlled using a custom-made humidifier and maintained at 47-55% which is above the efflorescence point of ammonium sulfate. Therefore, the liquid water content in seed particles in the humid experiments is expected to be higher than that in the dry experiments. However, it is noted that a diffusion dryer was placed before the particle sampling inlet to remove liquid water from the particles in order to eliminate its influence on calculating the change of organic particle volume/mass concentration. In all experiments, monoterpene concentration was measured using a gas chromatograph with flame ionization detector (GC-FID, SRI 8610C) equipped with a Tenax TA trap sampled at a rate of 0.14 L min^{-1} for 3 min. SO_2 and O_3 were measured by SO_2 analyzer (Model 43i, Thermo Scientific) and O_3 analyzer (Model 49i, Thermo Scientific), respectively. Particle size distribution and volume concentration were monitored using a custom-built scanning mobility particle sizer (SMPS) with a differential mobility analyzer (TSI 3081) and a condensation particle counter (TSI 3772). Relative humidity and temperature were monitored using an RH/T transmitter (HX94C, Omega). The temperature was monitored to be 23 $\pm$ 2 °C. To maintain a positive pressure inside the chamber, a 1 L min^{-1} dilution flow was added to balance the total sampling flow. Each experiment lasted for 4-5 h. Particle loss (including particle wall loss and dilution) in the chamber was corrected in a

size-dependent manner assuming first-order loss within each particle size bin, and the loss rate was
135 measured at the end of each experiment. Initial conditions and results are summarized in Table 1. It is noted that no correction for semivolatile vapor wall loss was made in the chamber experiments in this study. Therefore, the absolute values for SOA yields may be underestimated (Zhang et al., 2014). However, with relatively high seed area concentrations (1535-3309 μm^2 cm^{-3}) and volume concentrations (45-122 μm^3 cm^{-3}) used in this study, effects of vapor wall loss are expected to be similar across different
140 experiments and may not be important for relative SOA yield comparison. For example, similar SOA yields were observed when the injected seed volume concentration ranged from 47 to 82 μm^3 cm^{-3} for Exp. #1-3, and 59 to 71 μm^3 cm^{-3} for Exp. #11-13.

2.2 Flow tube experiments

To collect sufficient SOA mass for offline chemical analysis, SOA was also produced in a quartz flow
145 tube by reacting limonene or α-pinene with ozone (~3 ppm) in the presence or absence of SO_2 under dry (10-13% RH) and humid (55-60% RH) conditions. The flow tube has a diameter of 10.2 cm and length of 120 cm, and the residence time in the flow tube is 4 min. Cyclohexane was used as OH scavenger. Limonene/cyclohexane (1:1500 v/v) and α-pinene/cyclohexane solution (1:500 v/v) was prefilled in a 1mL syringe (Hamilton) and injected into the flow tube using a syringe pump (Legato 100, KDS). Two
150 injection ratios of limonene and SO_2 (500 ppb/250 ppb and 500 ppb/100 ppb) were used to investigate the effects of SO_2 on SOA formation. No seed aerosol was used during SOA formation to eliminate the influence of inorganic salt on chemical analysis, particularly that of sulfate. SOA was collected onto pre-baked quartz filters for 24 h. Filters were stored at -20°C prior to analysis and extracted in 5 mL HPLC-grade methanol (>99.9%, Caledon Laboratories Ltd.) by sonication for 10 min. The extract was filtered
155 using a 0.2 μm pore size syringe filter and prepared for composition analysis or peroxide quantification.

2.3 Chemical Characterization of SOA by ESI-IMS-TOF

Prior to chemical analysis, the SOA extract was concentrated to 0.5-1 mg mL^{-1} under a gentle N_2 stream in an evaporator (N-EVAP, Organomation). Particle composition was analyzed using electrospray ionization-ion mobility spectrometry-high resolution time-of-flight mass spectrometry (ESI-IMS-ToF,

160 TOFWERK, hereafter referred to as IMS-TOF) with a mass spectral resolution of 3500-4000 FWHM at m/z 250. Mass calibration was performed before each measurement with a mass accuracy within 5 ppm of each calibration chemical. Details of the IMS-TOF technique are described in recent publications by Krechmer et al. (2016) and Zhang et al., (2016). Briefly, SOA solution was introduced into IMS-TOF using direct infusion with a syringe pump (Legato 100, KDS) at 1-2 µL min^{-1}. Organic compounds in the

165 SOA extract were ionized by ESI in the negative mode. Ion droplets were evaporated in a desolvation tube and then separated in the ion drift tube based on ion mobility. The ion mobility (K) of an organic compound is a function of its molecular structure and ion-neutral interactions with N_2 buffer gas, and is calculated by measuring the drift time (t_d) in the IMS drift tube:

170 $$K = \frac{1}{t_d}\frac{L_d^2}{V_d}$$

where L_d is the length of the drift tube (20.5 cm) and V_d is the drift voltage (-9600 V). In all analyses, the desolvation tube and the ion drift tube were maintained at 333 ± 2 K and atmospheric pressure (~1000 mbar). Generally, small and compact molecules have shorter ion drift times and higher ion mobilities than

175 large and elongated molecules. One key feature of the IMS-TOF is that collision induced dissociation (CID) with nitrogen gas can be introduced between the ion drift tube and the time of flight region. CID analysis allows for attributing a fragment ion to its parent ion, as they share the same ion drift time (Zhang et al., 2016). Post-processing was performed with an Igor-based data analysis package (Tofware V2.5.7, TOFWERK).

180 **2.4 Quantification of peroxides in SOA**

Peroxide content in SOA was quantified using an iodometric-spectrophotometric method adapted from Docherty et al. (2005). Briefly, the iodide ion (I$^-$) can be oxidized by a peroxide moiety (including H_2O_2, ROOH and ROOR) to form I_2 under acidic conditions. I_2 then complexes with I$^-$ to form I_3^-. I_3^- is an orange-brown color complex which absorbs strongly at 470 nm.

185

$$\text{Peroxide} \ + \ \text{I}^- \ \xrightarrow{\text{Acid}} \ \text{I}_2 \ \xrightarrow{\text{I}^-} \ \text{I}_3^-$$
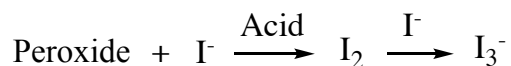
Peroxide content was measured for limonene SOA formed under humid conditions. Limonene SOA (LSOA) extract was concentrated to around 2 mg mL^{-1} and added into a 96 well UV plate (160 µL/well,

190   No. 655801, Greiner Bio-One). 20 µL Formic acid ($\geq$98%, Sigma-Aldrich) and 20 µL 0.1 g mL^{-1} potassium iodide (KI) solution were added to initiate reaction. KI solution was prepared by dissolving KI ($\geq$99%, Sigma-Aldrich) into MilliQ water (18.2 MΩ·cm). The plate was sealed with a UV transparent film (EdgeBio) to eliminate contact with ambient O_2. After 1 h at room temperature, the absorbance of the solution was measured using an absorbance plate reader (SpectraMax 190, Molecular Devices) at 470

195   nm. The absorbance signal was calibrated using benzoyl peroxide, and converted to a mass fraction assuming a MW of 242.23 g mol^{-1} (same as benzoyl peroxide). Background absorbance from a negative control (160 µL methanol + 20 µL formic acid + 20 µL KI) was subtracted from all reported absorbances. Each measurement was repeated at least two times.

200   **2.5 Bulk solution SO$_2$ bubbling experiments**

In addition to chamber and flow tube experiments, the reaction of SO_2 with peroxides was also investigated in bulk solutions. LSOA was collected from flow tube experiments mentioned previously and extracted using a methanol/H_2O (1:1) solution. The solution was divided into two and added into glass bottles. SO_2 (5.2 ppm balanced by N_2) was bubbled through one of the solutions at a flowrate of

205   0.02 L min^{-1} for 2.5 h. N_2 was bubbled through the other solution in parallel for 2.5 h at the same flow rate as a negative control. The total peroxide content was measured using the iodometric-spectrophotometric method mentioned in previous section and compared between the two solutions. As a positive control, a solution of 2-Butanone peroxide (technical grade, Sigma-Aldrich) was also bubbled with SO_2 and N_2 in parallel in the same manner.

210

2.6 Chamber experiments with SO$_3$

Experiments were also conducted to investigate the reactivity of SO_3 with organic compounds. The chamber was cleaned and filled with limonene (63 ppb) before experiment. Relative humidity in the chamber was maintained at 10-12%, which is similar to the LSOA experiments under dry conditions in Table 1 (Exp. #4-10). SO_3 was generated by blowing fuming sulfuric acid (20% free SO_3 basis, Sigma-Aldrich) into the chamber. Briefly, 0.2 mL fuming sulfuric acid was injected into a glass vessel and then blown with dry N_2 flow with a flow rate < 5 L min^{-1}. The upper limit of SO_3 injected into the chamber was estimated to be around 24 ppm.

3. Results and Discussion

3.1 SO_2 decay and limonene SOA formation under dry conditions (RH < 16%)

Reactions of SO_2 and SOA formation from limonene ozonolysis were investigated through experiments with and without SO_2. Synergistic effects were observed between LSOA formation and SO_2 oxidation, as SO_2 was consumed at the same time scales as the formation of LSOA. As shown in Fig. 1, as soon as ozone was added into the chamber prefilled with limonene and SO_2 at $t = 0$, concentrations of limonene and SO_2 began to decrease simultaneously, and particle concentration began to increase, suggesting that limonene ozonolysis produces intermediates that react with SO_2. After about 100 min, limonene concentrations were below detection limits, and both SO_2 consumption and particle formation began to slow down. In order to confirm that limonene was needed to produce the intermediates reactive towards SO_2, more limonene was added into the chamber at $t = 175$ min and both SO_2 consumption and particle formation resumed immediately. Tests have also been performed by injecting ozone in two separate batches into the chamber prefilled with limonene, as shown in Fig. S1. Similar to the experiments conducted under ozone-rich conditions (e.g. Fig. 1), synergistic effects have been observed. We therefore infer from the correlation between depletion rate of SO_2 and particle formation that similar species or processes are responsible for SO_2 reaction and LSOA formation.

When comparing SOA formation across different experiments under dry conditions (as shown in Fig. 2), we observed that aerosol formation increased with increasing initial SO_2 concentration when initial $[SO_2]$

< 140 ppb. At initial [SO_2] > 140 ppb, it appears that SO_2 has no further effect on SOA yields with initial [Limonene] ~ 30 ppb. Here we expect that the observed enhancement in total aerosol formation by SO_2 is the result of formation and condensation of sulfuric acid and/or increased SOA formation owing to increased particle acidity (Gao et al., 2004; Jang et al., 2002). Based on the measured loss of SO_2, we calculate the maximum contribution of condensed sulfuric acid to the increased aerosol mass by assuming all of the reacted SO_2 formed particle-phase sulfuric acid as a lower limit for SOA enhancement. As shown in Table 1, we compare two experiments (Exp. #1 and #7) in which similar amounts of limonene was consumed in the presence of 139 ppb of SO_2 (Exp. #7) and in the absence of SO_2 (Exp. #1). In Exp. #7, we observed a 5.7 ppb decay in SO_2 concentration, which would add a maximum of 14.7 μm^3 cm^{-3} to the particle volume concentration, assuming a density of 1.58 g cm^{-3} for an aqueous sulfuric acid solution under 10% RH (Heym, 1981). This amount of sulfuric acid can only account for 68% of the difference in particle volume between Exp. #7 and #1. There is still 32% of the enhancement of particle volume concentration that cannot be fully explained by introducing sulfate into the particle phase. Based on previous work demonstrating that acid catalysis by sulfuric acid increases SOA yields, we expect that SOA yields were enhanced as a result of increased particle acidity from condensation of sulfuric acid (Czoschke et al., 2003; Surratt et al., 2007).

3.2 SO_2 decay and limonene SOA formation under humid conditions (RH ~ 47-55%)

SO_2 reaction and SOA formation were also examined under humid conditions. As shown in Table 1 and Fig. 3A, an increase in particle volume concentration was also observed in the presence of SO_2 under humid conditions. However, the enhancements of particle volume concentration were smaller compared to those experiments conducted under dry conditions with similar initial conditions (e.g. Exp. #8 vs. Exp. #14, and Exp. #10 vs. Exp. #15). One of the possible reasons is that the formation of high-MW organic compounds and organosulfate is favored under high acidity conditions. The liquid water content in the particle phase under humid conditions is suggested to be higher than that under dry conditions as demonstrated in Section 2.1. Increased liquid water content reduces particle acidity through dilution and leads to decreased SOA enhancement. In addition, in all humid experiments, a diffusion dryer was used

before the SMPS particle sampling inlet to remove water and eliminate the influence of condensed water on particle volume concentration measurement. However, this may in turn lead to evaporation of semivolatile species, resulting in the smaller changes in the particle volume concentration. The loss of reactive intermediate onto the chamber walls may also play a role. We expect that the wall loss of reactive intermediates may be higher under humid conditions than under dry conditions (Loza et al., 2010). It should also be noted that in all the experiments, particle volume concentration instead of mass concentration was measured. Particle density may increase as its composition changes, leading to apparent changes in SOA yields.

On the other hand, greater SO_2 consumption was observed under humid conditions. For example, with an initial SO_2 concentration of 141 ppb, only 6 ppb of SO_2 was consumed under dry conditions (Exp. #8, Table 1 and Fig. 3B). Meanwhile, under humid conditions, the decay in SO_2 concentration was 15 ppb with a similar set of initial conditions (Exp. #14, Table 1 and Fig. 3B). The difference in amounts of SO_2 reacted and SOA yield enhancements between dry and humid conditions suggest that the mechanisms of the organic-SO_2 interactions are different between the two regimes. To identify these mechanisms, we conducted further experiments in which the experimental conditions were systematically varied to probe specific mechanisms.

3.3 Mechanisms of SO_2 reaction

3.3.1 Under dry conditions: Interaction between SO_2 and Criegee intermediates

Stabilized Criegee intermediates generated from alkene ozonolysis have been proposed to be important oxidants of SO_2 in the atmosphere (Mauldin III et al., 2012; Vereecken et al., 2012; Huang et al., 2015). The rates of bimolecular sCI reactions depend strongly on molecular structure. The reaction of CH_2OO with water and water dimer is rapid, with rate constants of $<1.5 \times 10^{-15}$ cm^3 s^{-1} and 6.5×10^{-12} cm^3 s^{-1} (Chao et al., 2015), respectively, and is likely the dominant sink of CH_2OO under almost all humidity conditions. However, Huang et al. demonstrated that $(CH_3)_2COO$, a di-substituted Criegee Intermediate has lower reaction rate constants with water and water dimer ($<1.5 \times 10^{-16}$ cm^3 s^{-1} and $<1.3 \times 10^{-13}$ cm^3 s^{-1}), suggesting that the reaction of a di-substituted sCI with SO_2 can be competitive with the water

reactions at atmospherically relevant RH. Since di-substituted sCIs can be produced from O_3 addition to either the endocyclic or exocyclic double bonds of limonene that yield sCI-1 and sCI-2, respectively (Scheme 1), we hypothesize that sCIs from limonene ozonolysis are responsible for the observed SO_2 decay under dry conditions.

To examine the contribution of sCI + SO_2 to the observed SO_2 consumption, formic acid was added as a sCI scavenger for both dry and humid experiments (Exp. #18-20). The initial concentration of formic acid added in these experiments was ~13 ppm. Based on the previously measured rate constant for reaction between sCIs from monoterpenes and formic acid (about 3 times higher than that of sCIs + SO_2) (Sipilä et al., 2014), we expect that at these formic acid concentrations, sCI + SO_2 reactions are minimized. As shown in Table 1 and Fig. S2 (see Supporting Information), much smaller SO_2 consumption was observed in the presence of 13 ppm of formic acid under dry conditions (Exp. #9 vs. Exp. #18, Table 1, Fig. S2A and S2B). This observation indicates without formic acid, the reaction with sCIs from monoterpene ozonolysis is a significant sink of SO_2. Results shown here are consistent with the observations from Sipilä et al. who demonstrated the importance of sCI + SO_2 reactions through measuring the production of sulfuric acid (Sipilä et al., 2014). Therefore, in the presence of SO_2, limonene ozonolysis can produce sCIs that can directly oxidize SO_2 to sulfuric acid, which may then proceed to enhance aerosol acidity and SOA formation, as discussed in Section 3.1.

3.3.2 Under humid conditions: Interaction between SO_2 and peroxides

On the other hand, under more humid conditions (RH~50%), SO_2 consumption did not decrease even in the presence of a large excess of formic acid (Exp. #18 vs. Exp. #19, Table 1, Fig. S2B and S2C), suggesting that, unlike sCIs from smaller precursors (e.g. dimethyl substituted sCIs (Huang et al., 2015a)), sCIs from monoterpenes is not an important sink for SO_2 under humid conditions. The SO_2 consumption remains significant and is even greater than under dry conditions, pointing to a yet unidentified sink of SO_2 that involves other reactive intermediates from monoterpene ozonolysis.

Here we propose that organic peroxides and/or hydrogen peroxide contribute significantly to the observed
consumption of SO_2. To test this hypothesis, the total peroxide content in SOA produced in the presence
or absence of SO_2 was measured using the iodometric-spectrophotometric method mentioned previously
(Section 2.4). Shown in Fig. 4, the mass fraction of total peroxides in LSOA is (48 ± 6) % in the absence
of SO_2. When SO_2 is present during SOA formation (SO_2 : limonene = 250 ppb : 500 ppb), the peroxide
fraction decreases to (13 ± 1) %. To further confirm this interaction, bulk experiments were conducted
by bubbling SO_2 into a solution of LSOA extract. Shown in Fig. S3 (left panel), the peroxide fraction
decreased significantly after SO_2 was bubbled through the LSOA solution, when compared to the negative
control experiment using N_2 bubbling to account for potential evaporation and/or decomposition at room
temperature. As a positive control, experiments were conducted by bubbling SO_2 through a solution of 2-
butanone peroxide. Again, a significant decrease in the peroxide content was observed (Fig. S3, right
panel), confirming that organic peroxides are reactive towards SO_2.

Since the observed SO_2 decay is greater under humid conditions than dry conditions during the chamber
experiments and higher liquid water content is expected under humid conditions, it is likely that SO_2 first
dissolves into the aqueous particle and the reaction proceeds in the aqueous phase. It is well known that
the aqueous phase reaction of hydrogen peroxide is the dominant sink of SO_2 in the atmosphere (Seinfeld
and Pandis, 2006). However, to the best of the authors' knowledge, this work is the first experimental
chamber study to suggest organic peroxides from monoterpene ozonolysis in aqueous particles are
reactive towards SO_2 under atmospherically relevant RH conditions. With the iodometric-
spectrophotometric method used in this study, we cannot distinguish between different types of peroxides,
specifically ROOH and ROOR. Previous work has shown that ROOH are important products of
monoterpene ozonolysis and precursors to peroxyhemiacetal formation (Docherty et al., 2005; Tobias et
al., 2000) and a major component of SOA formed from low NOx photooxidation of many VOCs,
including isoprene (Surratt et al., 2006) and n-alkanes (Schilling Fahnestock et al., 2014). SOA from
reactions between isoprene and nitrate radicals has been shown to contain significant amounts of ROOR-
type peroxides (Ng et al., 2008). Further work should focus on the mechanisms and kinetics of reaction
between SO_2 and different types of organic peroxides, which are ubiquitous in the atmosphere.

3.3.3 Other mechanisms of SO$_2$ reactions: SO$_2$ + ozone, SO$_2$ + OH

Experiments were also conducted to rule out other possible explanations for SO$_2$ decay. Aqueous phase

350 SO$_2$ has been shown to react with dissolved ozone at appreciable rates at high pH (Seinfeld and Pandis, 2006). To rule out the reaction between SO$_2$ + ozone, formic acid (13 ppm to minimize sCI reactions), ammonium sulfate seed (246 μm^3 cm^{-3}, 4.9 × 10^4 # cm^{-3}), SO$_2$ (289 ppb) and ozone (485 ppb) were injected and kept in the chamber under humid conditions (50% RH) for 6 h. Over the course of the experiment, the change in [SO$_2$] was less than 1 ppb, which is within experimental uncertainty (Fig. S4A),

355 suggesting that reactions between SO$_2$ and ozone either in the gas or particle phase have negligible effects on SO$_2$ consumption. This is likely because that ammonium sulfate seed is slightly acidic. The pH value calculated based on the E-AIM Aerosol Thermodynamic Model for ammonium sulfate at 50% RH is ~5 (Clegg et al., 1998; Wexler and Clegg, 2002). Under this pH condition, SO$_2$ oxidation by ozone is slow and less favorable in the aqueous phase. It is noted that the pH value was estimated without considering

360 the partitioning of trace gases (i.e. NH$_3$). Even lower pH (i.e. higher acidity) would be yielded if taking into account this effect. In addition, unlike SO$_2$ oxidation in a cloud droplet, the liquid water content in ammonium sulfate particles is limited. Therefore, little SO$_2$ depletion was observed. Another potential sink of SO$_2$ is the gas-phase reaction with OH radicals, which may be produced from unimolecular decomposition of the Criegee Intermediate. We conducted experiments with an initial concentration of

365 30 ppb limonene, 68 ppm cyclohexane and 300 ppb SO$_2$. At these concentrations, reaction rate of cyclohexane and OH is calculated to be around 130 times higher than that of SO$_2$ and OH with $k_{cyclohexane+OH} = 6.97 \times 10^{-12}$ cm^3 molecule^{-1} s^{-1} (Atkinson and Arey, 2003) and $k_{SO_2+OH} = 1.2 \times 10^{-12}$ cm^3 molecule^{-1} s^{-1} (Atkinson et al., 2004). Therefore, under our experimental conditions, the role of OH reaction is minimized. To confirm that OH reactions are not important, the concentration of cyclohexane,

370 the OH scavenger, was doubled in additional limonene ozonolysis experiments (Exp. #7-8 vs. Exp. #16-

17). No decrease of SO_2 consumption was observed ((14 ± 2) % in Exp. #7-8 vs. (15 ± 1) % in Exp. #16-17), confirming that gas phase OH radicals play a minor role in SO_2 oxidation in this study.

3.4 Organosulfate formation

Reactions between organic and sulfur-containing compounds are illustrated by the observed formation of organosulfates in the presence of SO_2. Previous work has shown that the bisulfate ion can react with alcohol or epoxide to form organosulfates, and organosulfate formation may be enhanced by particle acidity (Surratt et al., 2008). In this work, organosulfates present in SOA were identified using ESI-IMS-TOF through elemental formulas that are calculated from high resolution m/z ratios, and by matching ion drift times to either of the two most abundant sulfate fragments (HSO_4^- and $CH_3SO_4^-$) in the mass spectra.

Shown in Fig. 5A and 5B, eight parent ion peaks were matched to HSO_4^- and $CH_3SO_4^-$ fragment ion peaks in LSOA. The mass-to-charge ratios of these ions are consistent with sulfate-containing elemental formulas, confirming the organosulfate moiety. In addition, the assigned organosulfate ions were further validated by identifying trends (C, CH_2, O, CH_2O and CO_2) in Kendrick mass defect plots (Walser et al., 2008), as shown in Fig. S5 and Table S1. For example, in Fig. 5C, the ion with m/z 297.0835 was observed to have the same IMS drift time as $CH_3SO_4^-$ (drift time = 30.14 ms), indicating that m/z 297.0835 is an organosulfate ion. The m/z ratio is also consistent with the molecular formula of $C_{10}H_{17}O_8S^-$, and falls within the trend lines of adding CH_2O and O groups in the Kendrick mass defect plots to other identified organosulfate parent ions (e.g. $C_9H_{15}O_7S^-$ and $C_{10}H_{17}O_7S^-$). These ions were present only when SO_2 was added during SOA formation.

It should be noted that the number of organosulfate ions identified increased with increasing SO_2 concentrations. Shown in Fig. S6, we were able to identify 8 organosulfate ions when LSOA was formed in the presence of 100 ppb of SO_2, and 16 organosulfate ions when SO_2 was 250 ppb. We also observed that the total signal fraction of these organosulfate ions increased, but since no authentic standards were available for quantification, no conclusions can be drawn about the difference in organosulfate amounts between the two experiments. By comparing ESI mass spectra, we observe that when SO_2 is present, there

is a significant decrease in signal fraction from the high-MW species (m/z 320-500) and an increase in the signal fraction from low-MW compounds (m/z 150-320). The change of MW distribution may be due to the formation of organosulfate, and/or the formation and/or the uptake of low-MW compounds. As shown in Fig. S5, all the identified organosulfates are within the mass range of m/z 150-320. Although the hygroscopicity of organosulfate is not known, the sulfuric acid produced in the experiments with SO_2 may take up water and encourage uptake of small water-soluble organics, such as peroxides, epoxides and small aldehydes, also leading to the change of MW distribution in the ESI mass spectrum. Formation of low-MW compounds is also possible in the experiments with SO_2. For example, peroxide may react with bisulfite in the particle phase instead of forming peroxyhemiacetals, that will affect MW distribution. In all experiments, the average carbon oxidation state (OSc = 2 O/C - H/C) of SOA was observed to increase with SO_2. It is noted that since the negative mode in ESI is sensitive only to acidic species, the effects of SO_2 on relative signal fractions and oxidation states observed here may only be valid for these species. It should also be noted that compared to chamber experiments, SOA formed in the flow tube may be less oxidized due to the short residence time. However, this does not affect our conclusions regarding the effects of SO_2 on the change of SOA composition. The observations of organosulfate formation and increased SOA oxidation state in the presence of SO_2, are still valid despite the differences in residence time between the chamber and the flow tube experiments.

3.6 Potential mechanisms of SOA yield enhancement: comparison to α-Pinene

As mentioned earlier, enhanced SOA formation was observed from limonene ozonolysis in the presence of SO_2. The relative signal fraction of high-MW products measured in the IMS-TOF was reduced compared to when SO_2 was not present, suggesting that SO_2 may reduce oligomer formation, which may decrease SOA yields. However, we also observe that the presence of SO_2 (which is then converted to sulfate via previously mentioned mechanisms) increases organosulfate formation, and the average carbon oxidation state of low-MW products also increases. Our results therefore suggest that for limonene ozonolysis, the effect of functionalization (formation of organosulfate and increase in oxidation state) exceeds that of decreased oligomerization, leading to an overall increase in SOA yields. It should be noted that previous studies have focused mostly on the effect of acidic sulfate on SOA yields, which likely

promotes both functionalization and oligomerization reactions. Here we show that while SO_2 leads to a decrease in oligomerization, but there is still an overall increase in SOA yields from limonene ozonolysis.

To further compare the effects of oligomerization and functionalization, SOA formation from α-pinene ozonolysis was examined in the presence of SO_2. The IMS-TOF mass spectra of α-pinene SOA (ApSOA) (Fig. S7) show a similar decrease in the high m/z signal fraction when SO_2 is present, suggesting that SO_2 has a similar effect of decreasing oligomerization in this system. However, unlike in limonene ozonolysis, α-pinene SOA yields did not change significantly under different SO_2 concentrations under both dry and humid conditions (Fig. 7 and Table 1). It is likely that any enhancement in SOA yield by SO_2 through functionalization is masked by reduced oligomerization. As a result, there is little overall change in SOA yields from α-pinene ozonolysis. It is likely that the difference between the two systems can be explained by the number of double bonds and the extent of functionalization. Limonene has two double bonds. If SO_2 prevents oligomerization of the first-generation products, these products can still react further with ozone to add another oxidized functional groups to form condensable products. As a comparison, α-pinene only have one double bond. The presence of SO_2 reduces oligomerization and limits enhancements in SOA yields.

Under dry conditions, SO_2 can be oxidized by sCI to SO_3, which may be reactive towards organic compounds and may change the formation mechanism of SOA. As shown in Fig. S4B, SO_3 reacted rapidly with H_2O to form sulfuric acid once injected, even at 11% RH, the lowest RH among all the experiments conducted. During the experiment, around 7 ppb (11% of initial) limonene was reacted, which can be attributed to the reactive uptake of limonene onto sulfuric acid seed. This is consistent with the experimental observation from Liggio and Li (2008) in which significant uptake of monoterpenes onto highly acidic seed was observed in chamber studies under various humidity conditions. It is noted that the SO_3 concentration was very high (estimated to be ~24 ppm) during this experiment, which can be inferred from the rapid formation of new particles (2.8×10^6 # cm^{-3} and volume concentration of 1.1×10^4 μm^3 cm^{-3}), which are likely nucleated sulfuric acid particles. The concentration of SO_3 used in this test (~24 ppm) was expected to be much higher than those generated in the experiments shown in Table

1 (an estimated upper limit of 60 ppb SO_3 formation with initial limonene concentration of 30 ppb, assuming that sCI yield is unity and sCI only reacts with SO_2). Therefore, it is likely that the reaction between SO_3 and organic compounds do not play an important role in SOA formation under the experimental conditions in this study.

4. Implications

Our combined experimental observations of SO_2 consumption and formation of LSOA and ApSOA suggest that both sCI and organic peroxides formed from monoterpene ozonolysis may play crucial roles in SO_2 oxidation under atmospherically relevant humidity levels. We propose the simplified mechanisms shown in Scheme 2 to summarize our findings. Under dry conditions, sCI reacted with SO_2 to form SO_3 which quickly reacts with water to form sulfuric acid. In the presence of sulfuric acid in the particle phase, SOA formation can be enhanced through acid-catalyzed reactions (Jang et al., 2002). At the same time, we observed reduced oligomerization for semivolatile oxidation products relative to increased low-MW compounds by SO_2. As more SO_2 was added, the formation of sulfuric acid was limited by the initial monoterpene concentration, resulting in little change in particle acidity and, consequently, SOA yields. On the other hand, under atmospherically relevant humidity conditions, most of the sCI is scavenged by water and/or water dimer, and the sCI + SO_2 reaction is likely insignificant. However, SO_2 can partition into aerosol liquid water to form HSO_3^-, and we present evidence to suggest that HSO_3^- can further react with organic peroxides produced from monoterpene ozonolysis. This mechanism is consistent with the greater SO_2 consumption observed under humid conditions, since more aerosol water was available for both SO_2 and peroxides to partition.

In order to evaluate the relative contributions of sCI and peroxides as reactive sinks for SO_2 in our experiments, we formulate a simplified kinetic model to attribute observed SO_2 loss to each process. We note that without detailed knowledge of the SO_2 uptake mechanisms, the heterogeneous reaction of SO_2 with condensed phase peroxide is simplified as a bimolecular reaction. This reaction may depend on many factors, such as aerosol pH, aerosol liquid water content, and ionic strength. Nonetheless, we use this simplified model to apportion the observed SO_2 loss under the experimental conditions employed in this

work to each process. In particular, we will use this model to illustrate the relative importance of the sCI reaction under the two different experimental RH. Results are shown in Fig. 8 and the details of the box model can be found in the supporting information (Section S7).

485   In this model, we calculated the relative contributions of the two pathways under two humidities (10% and 50%) and under two initial concentrations of SO_2. As our laboratory observation suggests, SO_2 consumption increases with increasing humidity (Fig. 8A and 8B). In the high SO_2 scenario (Fig. 8A, $[SO_2] > [limonene]$), both interactions with sCI and peroxide play important roles in SO_2 oxidation. A major fraction of SO_2 consumption can be attributed to the reaction with sCI under dry conditions. At

490   50% RH, the amount of SO_2 consumed by the sCI pathway drops slightly (from 3 to 2 ppb in this scenario). On the other hand, the relative importance of reactive uptake by peroxides become dominant at 50% RH, accounting for 87% of the total SO_2 consumption. In the low SO_2 emission scenario (Fig. 8B, $[SO_2] < [limonene]$), sCI does not react with SO_2 at appreciable amounts, owing to the competition from reactions with water and water dimer. Therefore, sCI chemistry does not contribute significantly to the

495   SO_2 sink, and SO_2 consumption is dominated by reactions with peroxides and other reactive intermediates. To identify when the transition from "low SO_2" to "high SO_2" occurs, simulations were performed for a range of SO_2 concentrations, shown in Fig. 8C. Based on these results, we identified that even at RH = 10%, sCI does not become an important sink of SO_2 until SO_2 exceeds 50 ppb (with 30 ppb limonene injection), and this threshold is likely greater than 500 ppb at RH = 50%. The reaction with

500   peroxides is modelled as a simplified bimolecular reaction to match the observed SO_2 decay in our experiments. Moving forward, more information about the reaction mechanism is needed to accurately model this reaction. In particular, the specific peroxide compounds that are reactive towards SO_2 need to be identified using advanced analytical techniques (Krapf et al., 2017; Reinnig et al., 2009). Also, since it is likely that the reaction is occurring in aqueous particles, the Henry's Law constant of the peroxide

505   compounds will need to be measured. Despite these missing parameters, our simplified model highlights the importance of the reactive uptake pathway, and suggests further studies are warranted to elucidate the reaction rates and mechanisms for this reaction.

Currently, as a result of air quality control policies, SO_2 concentrations have significantly decreased in many areas in the world during the past decades. For example, the annual national average SO_2 concentration has dropped to < 10 ppb in the U.S. (U.S. EPA, 2013) and 1.3 ppb in Canada (ECCC, 2016). However, high SO_2 concentrations can still be observed, especially in some hot spots in North America such as near oil sands operations in Northern Alberta (Hazewinkel et al., 2008), and in developing countries like China where coal combustion is the main energy source. Hourly SO_2 concentrations frequently exceed 100 ppb in some megacities in China during the winter season (Lin et al., 2011, Zhang et al., 2015). Recent studies have shown that during heavy haze episodes, the rapid oxidation of SO_2 to sulfate cannot be explained by known mechanisms (Guo et al., 2014; Wang et al., 2014), and while heterogeneous reaction mechanisms have been proposed (Wang et al., 2016) , these mechanisms require relatively high pH to be plausible. Based on our experimental observations of SO_2 decay, we estimate that the uptake coefficient of SO_2 on the aqueous particle through reacting with peroxides from limonene ozonolysis is $1\text{-}5 \times 10^{-5}$ (Supporting Information, Section S8). These values are comparable to those from heterogeneous uptake of SO_2 on mineral aerosol (Huang et al., 2015b, 2014; Adams et al., 2005; Ullerstam et al., 2003) and sea salt (Gebel et al., 2000). It should be noted that organic peroxides are ubiquitous in different SOA systems and can be formed from oxidation by OH (Surratt et al., 2006; Yee et al., 2012), O_3 (Docherty et al., 2005) and NO_3 (Ng et al., 2008). Results from our study therefore suggest a new pathway of SO_2 oxidation in the atmosphere, which may contribute to the missing mechanisms of high-sulfate production in the polluted areas. Future work should investigate the role of peroxides from different SOA systems in oxidizing SO_2 and the atmospheric importance of these reactions.

The importance of the reaction pathways (sCI and reactive uptake) proposed in this study imply that oxidation of VOCs and reactions of SO_2 are tightly coupled. It is important to note that SO_2, the precursor to sulfate, can directly influence the chemistry of SOA formation. And the oxidation of monoterpenes provides viable pathways to act as SO_2 sinks and a source for sulfate in the atmosphere. Therefore, oxidation of VOCs and SO_2 must be considered holistically in order to fully understand the impacts of anthropogenic emissions on atmospheric chemistry.

Acknowledgement

This work was funded by Natural Sciences and Engineering Research Council and Canadian Foundation for Innovation. JY would like to acknowledge financial support from the Ontario Trillium Scholarship. The authors would like to thank Dr. Barbara Turpin and Dr. Hui-Ming Hung for insightful comments on heterogeneous uptake of SO_2 onto aqueous particles and thank Dr. John Liggio for helpful discussion with the SO_3 experiments.

Reference

Adams, J. W., Rodriguez, D. and Cox, R. A.: The uptake of SO_2 on Saharan dust: a flow tube study, Atmos. Chem. Phys., 5(10), 2679–2689, doi:10.5194/acp-5-2679-2005, 2005.

Atkinson, R. and Arey, J.: Atmospheric degradation of volatile organic compounds, Chem. Rev., 103(12), 4605–4638, doi:10.1021/cr0206420, 2003.

Atkinson, R., Baulch, D. L., Cox, R. a., Crowley, J. N., Hampson, R. F., Hynes, R. G., Jenkin, M. E., Rossi, M. J. and Troe, J.: Evaluated kinetic and photochemical data for atmospheric chemistry: Part 1 - gas phase reactions of Ox, HOx, NOx and SOx species, Atmos. Chem. Phys., 4, 1461–1738, doi:10.5194/acp-4-1461-2004, 2004.

Berndt, T., Richters, S., Kaethner, R., Voigtländer, J., Stratmann, F., Sipilä, M., Kulmala, M. and Herrmann, H.: Gas-phase ozonolysis of cycloalkenes: formation of highly oxidized RO_2 radicals and their reactions with NO, NO_2, SO_2, and other RO_2 radicals, J. Phys. Chem. A, 119(41), 10336–10348, doi:10.1021/acs.jpca.5b07295, 2015.

Brock, C. A., Washenfelder, R. A., Trainer, M., Ryerson, T. B., Wilson, J. C., Reeves, J. M., Huey, L. G., Holloway, J. S., Parrish, D. D., Hübler, G. and Fehsenfeld, F. C.: Particle growth in the plumes of coal-fired power plants, J. Geophys. Res. Atmos., 107(D12), 1–14, doi:10.1029/2001JD001062, 2002.

Calvert, J. G. and Stockwell, W. R.: Acid generation in the troposphere by gas-phase chemistry, Environ. Sci. Technol., 17(9), 428A–443A, doi:10.1021/es00115a002, 1983.

Carlton, A. G., Pinder, R. W., Bhave, P. V. and Pouliot, G. A.: To what extent can biogenic SOA be controlled?, Environ. Sci. Technol., 44(9), 3376–3380, doi:10.1021/es903506b, 2010.

Chao, W., Hsieh, J.-T., Chang, C.-H. and Lin, J. J.-M.: Direct kinetic measurement of the reaction of the

565 simplest Criegee intermediate with water vapor, Science, 347(6223), 751–754, doi:10.1126/science.1261549, 2015.

Clegg, S. L., Brimblecombe, P. and Wexler, A. S.: Thermodynamic model of the system $H^+-NH_4^+-SO_4^{2-}-NO_3^--H_2O$ at tropospheric temperatures, J. Phys. Chem. A, 102(12), 2137–2154, doi:10.1021/jp973042r, 1998.

570 Czoschke, N. M., Jang, M. and Kamens, R. M.: Effect of acidic seed on biogenic secondary organic aerosol growth, Atmos. Environ., 37(30), 4287–4299, doi:10.1016/S1352-2310(03)00511-9, 2003.

Docherty, K. S., Wu, W., Lim, Y. Bin and Ziemann, P. J.: Contributions of organic peroxides to secondary aerosol formed from reactions of monoterpenes with O_3, Environ. Sci. Technol., 39(11), 4049–4059, doi:10.1021/es050228s, 2005.

575 Environment Canada and Climate Change: National ambient level of sulphur dioxide, [online] Available from: https://www.ec.gc.ca/indicateurs-indicators/default.asp?lang=en&n=307CCE5B-1, 2016.

Friedman, B., Brophy, P., Brune, W. H. and Farmer, D. K.: Anthropogenic sulfur perturbations on biogenic oxidation: SO_2 additions impact gas-phase OH oxidation products of α- and β-pinene, Environ. Sci. Technol., 50(3), 1269–1279, doi:10.1021/acs.est.5b05010, 2016.

580 Gao, S., Ng, N. L., Keywood, M., Varutbangkul, V., Bahreini, R., Nenes, A., He, J., Yoo, K. Y., Beauchamp, J. L., Hodyss, R. P., Flagan, R. C. and Seinfeld, J. H.: Particle phase acidity and oligomer formation in secondary organic aerosol, Environ. Sci. Technol., 38(24), 6582–6589, doi:10.1021/es049125k, 2004.

Gebel, M. E., Finlayson-Pitts, B. J. and Ganske, J. A.: The uptake of SO_2 on synthetic sea salt and some
585 of its components, Geophys. Res. Lett., 27(6), 887–890, doi:10.1029/1999GL011152, 2000.

Goldstein, A. H., Koven, C. D., Heald, C. L. and Fung, I. Y.: Biogenic carbon and anthropogenic pollutants combine to form a cooling haze over the southeastern United States., Proc. Natl. Acad. Sci., 106(22), 8835–8840, doi:10.1073/pnas.0904128106, 2009.

de Gouw, J. A., Middlebrook, A. M., Warneke, C., Goldan, P. D., Kuster, W. C., Roberts, J. M.,
590 Fehsenfeld, F. C., Worsnop, D. R., Canagaratna, M. R., Pszenny, A. A. P., Keene, W. C., Marchewka, M., Bertman, S. B. and Bates, T. S.: Budget of organic carbon in a polluted atmosphere: Results from the New England Air Quality Study in 2002, J. Geophys. Res. Atmos., 110(D16),

doi:10.1029/2004JD005623, 2005.

Guo, S., Hu, M., Zamora, M. L., Peng, J., Shang, D., Zheng, J., Du, Z., Wu, Z., Shao, M., Zeng, L., Molina, M. J. and Zhang, R.: Elucidating severe urban haze formation in China, Proc. Natl. Acad. Sci. , 111(49), 17373–17378, doi:10.1073/pnas.1419604111, 2014.

Hazewinkel, R. R. O., Wolfe, A. P., Pla, S., Curtis, C. and Hadley, K.: Have atmospheric emissions from the Athabasca Oil Sands impacted lakes in northeastern Alberta, Canada?, Can. J. Fish. Aquat. Sci., 65(8), 1554–1567, doi:10.1139/F08-074, 2008.

He, H., Wang, Y., Ma, Q., Ma, J., Chu, B., Ji, D., Tang, G., Liu, C., Zhang, H. and Hao, J.: Mineral dust and NOx promote the conversion of SO_2 to sulfate in heavy pollution days, Sci. Rep., 4, 4172, doi:10.1038/srep04172, 2014.

Heald, C. L., Henze, D. K., Horowitz, L. W., Feddema, J., Lamarque, J.-F., Guenther, A., Hess, P. G., Vitt, F., Seinfeld, J. H., Goldstein, A. H. and Fung, I.: Predicted change in global secondary organic aerosol concentrations in response to future climate, emissions, and land use change, J. Geophys. Res. Atmos., 113(D5), doi:10.1029/2007JD009092, 2008.

Heym, C.: Fluorescence histochemistry of biogenic monoamines, in Techniques in neuroanatomical research, edited by C. Heym and W.-G. Forssmann, p. 142, Springer, Berlin, Heidelberg., 1981.

Huang, H.-L., Chao, W. and Lin, J. J.-M.: Kinetics of a Criegee intermediate that would survive high humidity and may oxidize atmospheric SO_2, Proc. Natl. Acad. Sci., 112(35), 10857–10862, doi:10.1073/pnas.1513149112, 2015a.

Huang, L., Zhao, Y., Li, H. and Chen, Z.: Kinetics of heterogeneous reaction of sulfur dioxide on authentic mineral dust: effects of relative humidity and hydrogen peroxide, Environ. Sci. Technol., 49(18), 10797–10805, doi:10.1021/acs.est.5b03930, 2015b.

Huang, X., Song, Y., Zhao, C., Li, M., Zhu, T., Zhang, Q. and Zhang, X.: Pathways of sulfate enhancement by natural and anthropogenic mineral aerosols in China, J. Geophys. Res. Atmos., 119(24), 14,114-165,179, doi:10.1002/2014JD022301, 2014.

Hung, H. M. and Hoffmann, M. R.: Oxidation of gas-phase SO_2 on the surfaces of acidic microdroplets: implications for sulfate and sulfate radical anion formation in the atmospheric liquid phase, Environ. Sci. Technol., 49(23), 13768–13776, doi:10.1021/acs.est.5b01658, 2015.

Iinuma, Y., Müller, C., Böge, O., Gnauk, T. and Herrmann, H.: The formation of organic sulfate esters in the limonene ozonolysis secondary organic aerosol (SOA) under acidic conditions, Atmos. Environ., 41(27), 5571–5583, doi:10.1016/j.atmosenv.2007.03.007, 2007.

Jang, M., Czoschke, N. M., Lee, S. and Kamens, R. M.: Heterogeneous atmospheric aerosol production by acid-catalyzed particle-phase reactions, Science, 298(5594), 814–817, doi:10.1126/science.1075798, 2002.

Jimenez, J. L., Canagaratna, M. R., Donahue, N. M., Prevot, A. S. H., Zhang, Q., Kroll, J. H., DeCarlo, P. F., Allan, J. D., Coe, H., Ng, N. L., Aiken, A. C., Docherty, K. S., Ulbrich, I. M., Grieshop, A. P., Robinson, A. L., Duplissy, J., Smith, J. D., Wilson, K. R., Lanz, V. A., Hueglin, C., Sun, Y. L., Tian, J., Laaksonen, A., Raatikainen, T., Rautiainen, J., Vaattovaara, P., Ehn, M., Kulmala, M., Tomlinson, J. M., Collins, D. R., Cubison, M. J., Dunlea, E. J., Huffman, J. A., Onasch, T. B., Alfarra, M. R., Williams, P. I., Bower, K., Kondo, Y., Schneider, J., Drewnick, F., Borrmann, S., Weimer, S., Demerjian, K., Salcedo, D., Cottrell, L., Griffin, R., Takami, A., Miyoshi, T., Hatakeyama, S., Shimono, A., Sun, J. Y., Zhang, Y. M., Dzepina, K., Kimmel, J. R., Sueper, D., Jayne, J. T., Herndon, S. C., Trimborn, A. M., Williams, L. R., Wood, E. C., Middlebrook, A. M., Kolb, C. E., Baltensperger, U., Worsnop, D. R., Worsnop, D. R., Dunlea, J., Huffman, J. A., Onasch, T. B., Alfarra, M. R., Williams, P. I., Bower, K., Kondo, Y., Schneider, J., Drewnick, F., Borrmann, S., Weimer, S., Demerjian, K., Salcedo, D., Cottrell, L., Griffin, R., Takami, A., Miyoshi, T., Hatakeyama, S., Shimono, A., Sun, J. Y., Zhang, Y. M., Dzepina, K., Kimmel, J. R., Sueper, D., Jayne, J. T., Herndon, S. C., Trimborn, A. M., Williams, L. R., Wood, E. C., Middlebrook, A. M., Kolb, C. E., Baltensperger, U. and Worsnop, D. R.: Evolution of organic aerosols in the atmosphere, Science, 326(5959), 1525–1529, doi:10.1126/science.1180353, 2009.

Kan, C. S., Calvert, J. G. and Shaw, J. H.: Oxidation of sulfur dioxide by methylperoxy radicals, J. Phys. Chem., 85(9), 1126–1132, doi:10.1021/j150609a011, 1981.

Krapf, M., El Haddad, I., Bruns, E. A., Molteni, U., Daellenbach, K. R., Prévôt, A. S. H., Baltensperger, U. and Dommen, J.: Labile peroxides in secondary organic aerosol, Chem, 1(4), 603–616, doi:10.1016/j.chempr.2016.09.007, 2017.

Krechmer, J. E., Groessl, M., Zhang, X., Junninen, H., Massoli, P., Lambe, A. T., Kimmel, J. R., Cubison, M. J., Graf, S., Lin, Y., Budisulistiorini, S. H. and Zhang, H.: Ion mobility spectrometry – mass

spectrometry (IMS – MS) for on- and offline analysis of atmospheric gas and aerosol species, Atmos.

650   Meas. Tech., 9, 3245–3262, doi:10.5194/amt-9-3245-2016, 2016.

Liggio, J. and Li, S.-M.: Reversible and irreversible processing of biogenic olefins on acidic aerosols, Atmos. Chem. Phys., 8(7), 2039–2055, doi:10.5194/acp-8-2039-2008, 2008.

Lin, W., Xu, X., Ge, B. and Liu, X.: Gaseous pollutants in Beijing urban area during the heating period 2007–2008: variability, sources, meteorological, and chemical impacts, Atmos. Chem. Phys., 11(15),

655   8157–8170, doi:10.5194/acp-11-8157-2011, 2011.

Liu, S., Jia, L., Xu, Y., Tsona, N. T., Ge, S. and Du, L.: Photooxidation of cyclohexene in the presence of SO_2: SOA yield and chemical composition, Atmos. Chem. Phys., 17(21), 13329–13343, doi:10.5194/acp-17-13329-2017, 2017.

Loza, C. L., Chan, A. W. H., Galloway, M. M., Keutsch, F. N., Flagan, R. C. and Seinfeld, J. H.:

660   Characterization of vapor wall loss in laboratory chambers, Environ. Sci. Technol., 44(13), 5074–5078, doi:10.1021/es100727v, 2010.

Marais, E. A., Jacob, D. J., Turner, J. R. and Mickley, L. J.: Evidence of 1991 – 2013 decrease of biogenic secondary organic aerosol in response to SO_2 emission controls, Environ. Res. Lett., 12(5), 54018, doi:https://doi.org/10.1088/1748-9326/aa69c8, 2017.

665   Mauldin III, R. L., Berndt, T., Sipilä, M., Paasonen, P., Petäjä, T., Kim, S., Kurtén, T., Stratmann, F., Kerminen, V.-M. and Kulmala, M.: A new atmospherically relevant oxidant of sulphur dioxide, Nature, 488(7410), 193–196, doi:10.1038/nature11278, 2012.

McLinden, C. A., Fioletov, V., Shephard, M. W., Krotkov, N., Li, C., Martin, R. V., Moran, M. D. and Joiner, J.: Space-based detection of missing sulfur dioxide sources of global air pollution, Nat. Geosci.,

670   9(7), 496–500, doi:10.1038/ngeo2724, 2016.

Ng, N. L., Chhabra, P. S., Chan, A. W. H., Surratt, J. D., Kroll, J. H., Kwan, A. J., McCabe, D. C., Wennberg, P. O., Sorooshian, A., Murphy, S. M., Dalleska, N. F., Flagan, R. C. and Seinfeld, J. H.: Effect of NOx level on secondary organic aerosol (SOA) formation from the photooxidation of terpenes, Atmos. Chem. Phys., 7(19), 5159–5174, doi:10.5194/acp-7-5159-2007, 2007.

675   Ng, N. L., Kwan, A. J., Surratt, J. D., Chan, A. W. H., Chhabra, P. S., Sorooshian, A., Pye, H. O. T., Crounse, J. D., Wennberg, P. O., Flagan, R. C. and Seinfeld, J. H.: Secondary organic aerosol (SOA)

formation from reaction of isoprene with nitrate radicals (NO_3), Atmos. Chem. Phys., 8(14), 4117–4140, doi:10.5194/acp-8-4117-2008, 2008.

Passananti, M., Kong, L., Shang, J., Dupart, Y., Perrier, S., Chen, J., Donaldson, D. J. and George, C.:
680 Organosulfate formation through the heterogeneous reaction of sulfur dioxide with unsaturated fatty acids and long-chain alkenes, Angew. Chemie Int. Ed., 55(35), 10336–10339, doi:10.1002/anie.201605266, 2016.

Reinnig, M.-C., Warnke, J. and Hoffmann, T.: Identification of organic hydroperoxides and hydroperoxy acids in secondary organic aerosol formed during the ozonolysis of different monoterpenes and
685 sesquiterpenes by on-line analysis using atmospheric pressure chemical ionization ion trap mass spectrom, Rapid Commun. Mass Spectrom., 23(11), 1735–1741, doi:10.1002/rcm.4065, 2009.

Richards-Henderson, N. K., Goldstein, A. H. and Wilson, K. R.: Sulfur dioxide accelerates the heterogeneous oxidation rate of organic aerosol by hydroxyl radicals, Environ. Sci. Technol., 50(7), 3554–3561, doi:10.1021/acs.est.5b05369, 2016.
690 Schilling Fahnestock, K. A., Yee, L. D., Loza, C. L., Coggon, M. M., Schwantes, R., Zhang, X., Dalleska, N. F. and Seinfeld, J. H.: Secondary organic aerosol composition from C12 alkanes, J. Phys. Chem. A, 119(19), 4281–4297, doi:10.1021/jp501779w, 2014.

Seinfeld, J. H. and Pandis, S. N.: Atmospheric chemistry and physics: from air pollution to climate change, 2nd Ed., Wiley: New York., 2006.
695 Shang, J., Passananti, M., Dupart, Y., Ciuraru, R., Tinel, L., Rossignol, S., Perrier, S., Zhu, T. and George, C.: SO_2 uptake on oleic acid: A new formation pathway of organosulfur compounds in the atmosphere, Environ. Sci. Technol. Lett., 3(2), 67–72, doi:10.1021/acs.estlett.6b00006, 2016.

Sipilä, M., Jokinen, T., Berndt, T., Richters, S., Makkonen, R., Donahue, N. M., Mauldin III, R. L., Kurtén, T., Paasonen, P., Sarnela, N., Ehn, M., Junninen, H., Rissanen, M. P., Thornton, J., Stratmann, F.,
700 Herrmann, H., Worsnop, D. R., Kulmala, M., Kerminen, V.-M. and Petäjä, T.: Reactivity of stabilized Criegee intermediates (sCIs) from isoprene and monoterpene ozonolysis toward SO_2 and organic acids, Atmos. Chem. Phys., 14(22), 12143–12153, doi:10.5194/acp-14-12143-2014, 2014.

Surratt, J. D., Murphy, S. M., Kroll, J. H., Ng, N. L., Hildebrandt, L., Sorooshian, A., Szmigielski, R., Vermeylen, R., Maenhaut, W., Claeys, M., Flagan, R. C. and Seinfeld, J. H.: Chemical composition of

705   secondary organic aerosol formed from the photooxidation of isoprene, J. Phys. Chem. A, 110(31), 9665–9690, doi:10.1021/jp061734m, 2006.

Surratt, J. D., Lewandowski, M., Offenberg, J. H., Kleindienst, T. E., Edney, E. O., Seinfeld, J. H. and Surratt, J. D.: Effect of acidity on secondary organic aerosol formation from isoprene, Environ. Sci. Technol., 41(15), 5363–5369, doi:10.1021/es0704176, 2007.

710   Surratt, J. D., Gómez-González, Y., Chan, A. W. H., Vermeylen, R., Shahgholi, M., Kleindienst, T. E., Edney, E. O., Offenberg, J. H., Lewandowski, M., Jaoui, M., Maenhaut, W., Claeys, M., Flagan, R. C. and Seinfeld, J. H.: Organosulfate formation in biogenic secondary organic aerosol, J. Phys. Chem. A, 112(36), 8345–8378, doi:10.1021/jp802310p, 2008.

Szidat, S., Jenk, T. M., Synal, H. A., Kalberer, M., Wacker, L., Hajdas, I., Kasper-Giebl, A. and
715   Baltensperger, U.: Contributions of fossil fuel, biomass-burning, and biogenic emissions to carbonaceous aerosols in Zurich as traced by ^{14}C, J. Geophys. Res. Atmos., 111(7), 1–12, doi:10.1029/2005JD006590, 2006.

Tobias, H. J., Docherty, K. S., Beving, D. E. and Ziemann, P. J.: Effect of relative humidity on the chemical composition of secondary organic aerosol formed from reactions of 1-tetradecene and O_3,
720   Environ. Sci. Technol., 34(11), 2116–2125, doi:10.1021/es991057s, 2000.

Tolocka, M. P., Jang, M., Ginter, J. M., Cox, F. J., Kamens, R. M. and Johnston, M. V: Formation of oligomers in secondary organic aerosol, Environ. Sci. Technol., 38(5), 1428–1434, doi:10.1021/es035030r, 2004.

U.S. Environmental Protection Agency: Air quality trends (1970-2012): sulfur dioxide concentrations,
725   [online] Available from: https://www3.epa.gov/region9/air/trends/so2-annual.html, 2013.

U.S. Environmental Protection Agency: National Summary of Sulfur Dioxide Emissions, [online] Available from: https://www3.epa.gov/cgi-bin/broker?polchoice=SO2&_debug=0&_service=data&_program=dataprog.national_1.sas, 2014.

Ullerstam, M., Johnson, M. S., Vogt, R. and Ljungström, E.: DRIFTS and Knudsen cell study of the
730   heterogeneous reactivity of SO_2 and NO_2 on mineral dust, Atmos. Chem. Phys., 3(6), 2043–2051, doi:10.5194/acp-3-2043-2003, 2003.

Vereecken, L., Harder, H. and Novelli, A.: The reaction of Criegee intermediates with NO, RO_2, and SO_2,

and their fate in the atmosphere, Phys. Chem. Chem. Phys., 14(42), 14682, doi:10.1039/c2cp42300f, 2012.

Walser, M. L., Desyaterik, Y., Laskin, J., Laskin, A. and Nizkorodov, S. A.: High-resolution mass
735   spectrometric analysis of secondary organic aerosol produced by ozonation of limonene, Phys. Chem. Chem. Phys., 10(7), 1009–1022, doi:10.1039/B712620D, 2008.

Wang, G., Zhang, R., Gomez, M. E., Yang, L., Levy Zamora, M., Hu, M., Lin, Y., Peng, J., Guo, S., Meng, J., Li, J., Cheng, C., Hu, T., Ren, Y., Wang, Y., Gao, J., Cao, J., An, Z., Zhou, W., Li, G., Wang, J., Tian, P., Marrero-Ortiz, W., Secrest, J., Du, Z., Zheng, J., Shang, D., Zeng, L., Shao, M., Wang, W.,
740   Huang, Y., Wang, Y., Zhu, Y., Li, Y., Hu, J., Pan, B., Cai, L., Cheng, Y., Ji, Y., Zhang, F., Rosenfeld, D., Liss, P. S., Duce, R. A., Kolb, C. E. and Molina, M. J.: Persistent sulfate formation from London Fog to Chinese haze, Proc. Natl. Acad. Sci. , 113(48), 13630–13635, doi:10.1073/pnas.1616540113, 2016.

Wang, Y., Zhang, Q., Jiang, J., Zhou, W., Wang, B., He, K., Duan, F., Zhang, Q., Philip, S. and Xie, Y.: Enhanced sulfate formation during China's severe winter haze episode in January 2013 missing from
745   current models, J. Geophys. Res. Atmos., 119(17), 10,410-425,440, doi:10.1002/2013JD021426, 2014.

Weber, R. J., Sullivan, A. P., Peltier, R. E., Russell, A., Yan, B., Zheng, M., de Grouw, J., Warneke, C., Brock, C., Holloway, J. S., Atlas, E. L. and Edgerton, E.: A study of secondary organic aerosol formation in the anthropogenic-influenced southeastern United States, J. Geophys. Res. Atmos., 112(13), 1–13, doi:10.1029/2007JD008408, 2007.

750   Welz, O., Savee, J. D., Osborn, D. L., Vasu, S. S., Percival, C. J., Shallcross, D. E. and Taatjes, C. A.: Direct kinetic measurements of Criegee intermediate (CH_2OO) formed by reaction of CH_2I with O_2, Science, 335(6065), 204–207, doi:10.1126/science.1213229, 2012.

Wexler, A. S. and Clegg, S. L.: Atmospheric aerosol models for systems including the ions H^+, NH_4^+, Na^+, SO_4^{2-}, NO_3^-, Cl^-, Br^-, and H_2O, J. Geophys. Res. Atmos., 107(D14), ACH 14-1-14-14,
755   doi:10.1029/2001JD000451, 2002.

Xu, L., Guo, H., Boyd, C. M., Klein, M., Bougiatioti, A., Cerully, K. M., Hite, J. R., Isaacman-VanWertz, G., Kreisberg, N. M., Knote, C., Olson, K., Koss, A., Goldstein, A. H., Hering, S. V, de Gouw, J., Baumann, K., Lee, S.-H., Nenes, A., Weber, R. J. and Ng, N. L.: Effects of anthropogenic emissions on aerosol formation from isoprene and monoterpenes in the southeastern United States, Proc. Natl. Acad.
760   Sci., 112(1), 37–42, doi:10.1073/pnas.1417609112, 2015.

Xue, J., Yuan, Z., Griffith, S. M., Yu, X., Lau, A. K. H. and Yu, J. Z.: Sulfate formation enhanced by a cocktail of high NOx, SO$_2$, particulate matter, and droplet pH during haze-fog events in megacities in China: an observation-based modeling investigation, Environ. Sci. Technol., 50(14), 7325–7334, doi:10.1021/acs.est.6b00768, 2016.

765 Ye, J., Gordon, C. A. and Chan, A. W. H.: Enhancement in secondary organic aerosol formation in the presence of preexisting organic particle, Environ. Sci. Technol., 50(7), 3572–3579, doi:10.1021/acs.est.5b05512, 2016.

Yee, L. D., Craven, J. S., Loza, C. L., Schilling, K. A., Ng, N. L., Canagaratna, M. R., Ziemann, P. J., Flagan, R. C. and Seinfeld, J. H.: Secondary organic aerosol formation from low-NOx photooxidation of

770 dodecane: evolution of multigeneration gas-phase chemistry and aerosol composition, J. Phys. Chem. A, 116(24), 6211–6230, doi:10.1021/jp211531h, 2012.

Zhang, X., Cappa, C. D., Jathar, S. H., McVay, R. C., Ensberg, J. J., Kleeman, M. J., Seinfeld, J. H. and Christopher D. Cappa: Influence of vapor wall loss in laboratory chambers on yields of secondary organic aerosol., Proc. Natl. Acad. Sci. U. S. A., 111(16), 1–6, doi:10.1073/pnas.1404727111, 2014.

775 Zhang, X., Krechmer, J., Groessl, M., Xu, W., Graf, S., Cubison, M., Jayne, J. T., Jimenez, J. L., Worsnop, D. R. and Canagaratna, M. R.: A novel framework for molecular characterization of atmospherically relevant organic compounds based on collision cross section and mass-to-charge ratio, Atmos. Chem. Phys., 16(20), 12945–12959, doi:10.5194/acp-16-12945-2016, 2016.
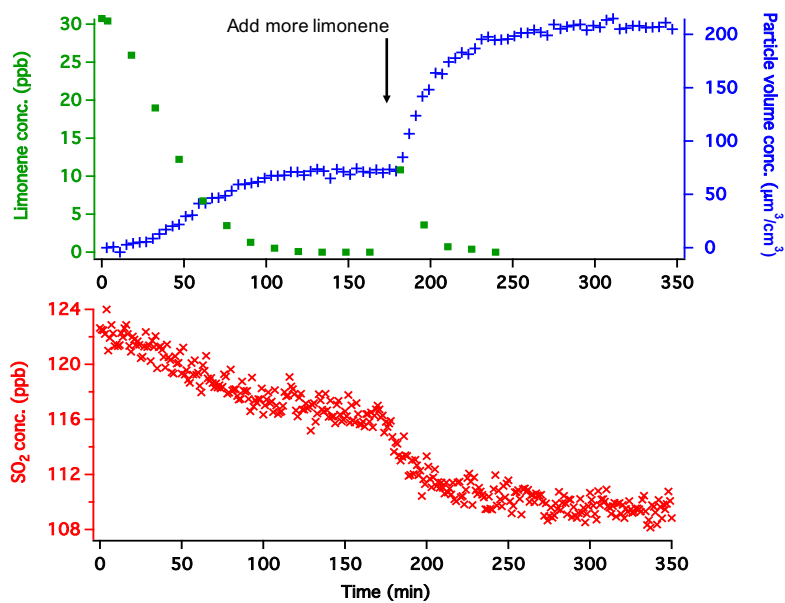
Figure 1 Particle volume concentration, limonene concentration and SO_2 concentration as a function of experimental time. After 105 min, the limonene concentration was below 1 ppb, and the particle volume concentration and SO_2 concentration began to stabilize. At $t = 170$ min, additional limonene was injected into the chamber, and particle formation and SO_2 decay resumed. The timescale of SO_2 consumption matches that of SOA formation suggesting that there are synergistic effects between LSOA formation and SO_2 oxidation.

785
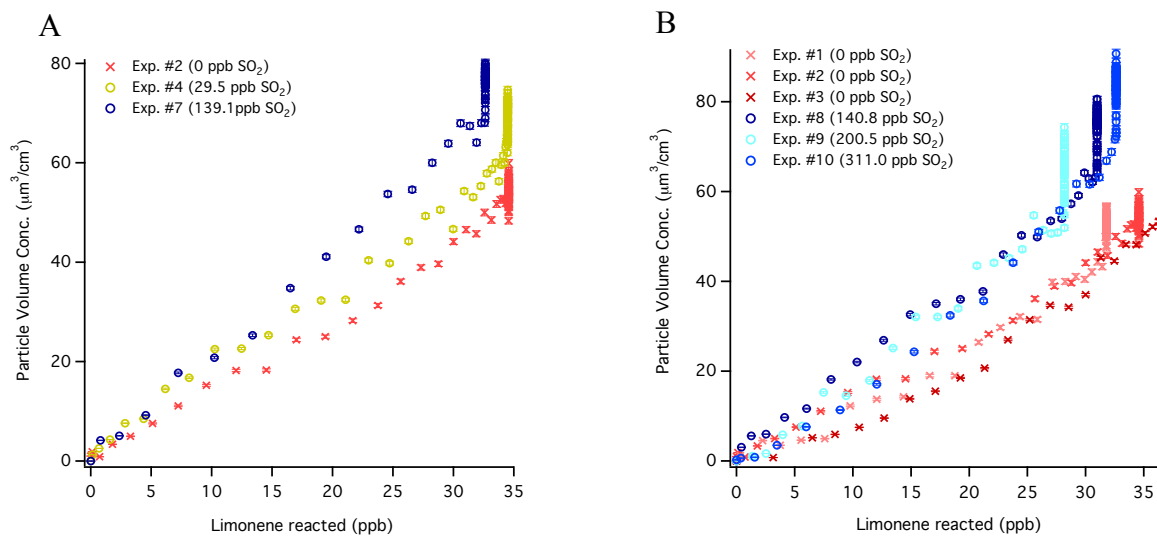
790

Figure 2 Growth of particle volume concentration as a function of limonene consumption under dry conditions. Particle concentration increased with increasing SO_2 injection concentration (0 ppb, 30 ppb and 139 ppb) under dry conditions (panel A). The enhancement reached a plateau as more SO_2 was injected (panel B).

795

Table 1 Summary of conditions and results for limonene and α-pinene SOA experiments

Exp. #	HC reacted (ppb)	Initial SO_2 conc. (ppb)	ΔSO_2 (ppb)	HCOOH (ppm)	Seed volume conc. [a] (μm^3 cm^{-3})	Final volume conc. [a] (μm^3 cm^{-3})	ΔM [b] (μg cm^{-3})	SOA yield	RH
Limonene									
1	31.8	0	0	0	67.0	121.9	71.4	39.6%	14%
2	34.6	0	0	0	82.3	137.3	71.5	36.5%	13%
3	36.5	0	0	0	46.9	110.7	82.9	40.1%	16%
4	34.5	29.5	2.7	0	59.8	132.1	94.0	48.1%	16%
5	31.1	110.3	5.2	0	46.8	116.9	91.1	51.7%	11%
6	30.4	122.2	5.9	0	65.5	136.8	92.7	53.8%	10%
7	31.0	139.1	5.7	0	89.8	166.3	99.5	56.6%	12%
8	32.6	140.8	6.1	0	42.9	119.9	100.1	54.2%	15%
9	28.2	200.5	5.5	0	122.6	193.1	91.7	57.4%	13%
10	32.6	311.0	7.3	0	68.2	151.5	108.3	58.6%	16%
11	31.5	0	0	0	68.1	115.1	61.1	34.2%	55%
12	37.3	0	0	0	59.0	118.3	77.0	36.4%	50%
13	38.4	0	0	0	70.9	125.8	71.4	32.8%	50%
14	33.7	144.3	15.5	0	57.4	110.5	69.0	36.1%	55%
15	27.8	308.8	15.2	0	78.5	130.0	67.0	42.5%	47%
16	35.0	137.4	7.4 [c]	0	56.9				16%
17	29.1	136.4	6.5 [c]	0	57.7				14%
18	34.7	251.6	2.2	13	65.0				12%
19	25.4	262.2	10.0	13	52.3				50%
20	28.3	605.4	12.4	13	117.5				52%
α-Pinene									
21	23.9	0	0	0	30.0	53.0	28.8	21.3%	14%
22	25.0	0	0	0	41.0	65.4	30.5	21.5%	14%
23	29.6	0	0	0	24.0	50.5	33.1	19.7%	12%
24	27.2	24.5	1.2	0	35.0	55.9	26.1	16.9%	13%
25	24.1	42.3	1.9	0	64.6	81.1	20.6	15.1%	10%
26	21.8	107.8	2.3	0	54.3	70.7	20.5	16.6%	12%
27	33.7	99.2	2.6	0	41.0	71.7	38.4	20.1%	12%
28	27.4	0	0	0	55.2	76.8	27.0	17.4%	49%
29	27.7	0	0	0	38.6	63.2	30.8	19.6%	48%
30	27.2	53.1	4.5	0	50.1	71.6	26.9	17.4%	46%

[a]: Volume concentrations after particle wall loss correction.

[b]: Particle mass concentration formed during the experiments (ΔM = (Final volume conc. - Seed volume conc.) $\times \rho$). A density of 1.30 and 1.25 g cm^{-3} was applied to calculate limonene and α-pinene SOA mass concentration, respectively.

800 [c]: Twice the amount of cyclohexane was added in Exp. #16 and #17 to examine the reaction between SO_2 and OH.

805

810
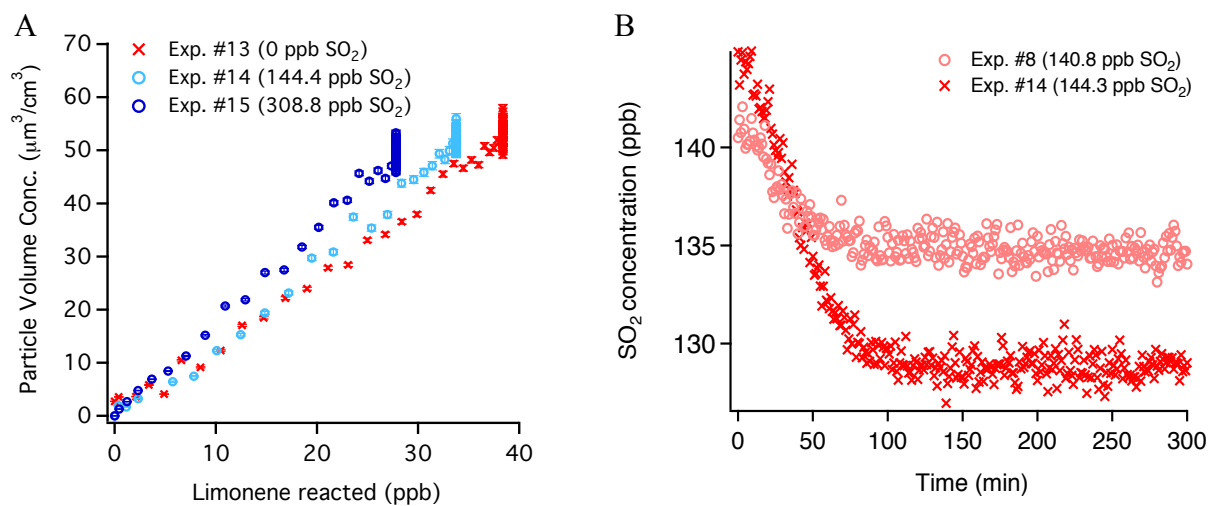
815 **Figure 3** A) Particle volume concentration as a function of limonene reacted under humid conditions. Enhanced particle mass formation was observed with increasing SO_2 concentration. B) Greater consumption of SO_2 was observed under humid conditions than under dry conditions. By comparing Exp. #14 (humid) and Exp. #8 (dry), with similar initial SO_2 concentration, SO_2 consumption was more than two times greater under humid conditions.

820
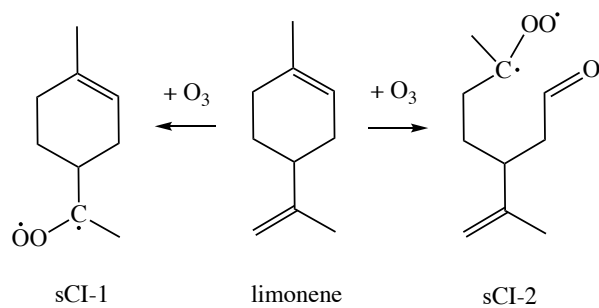
825

Scheme 1 Formation of di-substituted sCI from limonene ozonolysis

830
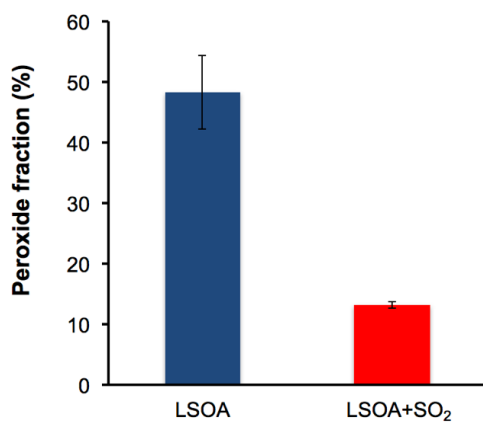
835 **Figure 4** Mass fraction of peroxides in LSOA formed in the presence and absence of SO_2. Error bars represent measurements of three LSOA and three LSOA + SO_2 filters collected from different experiments. Peroxide measurement for each filter was repeated two times.

A

B

840 C
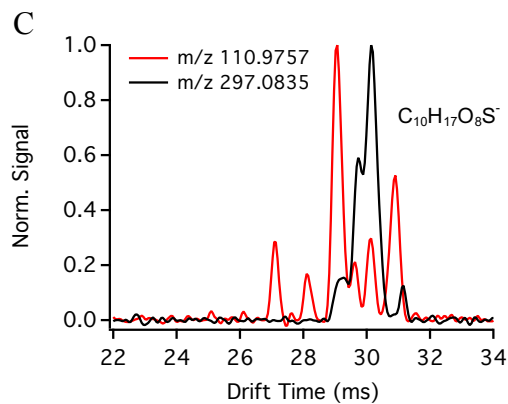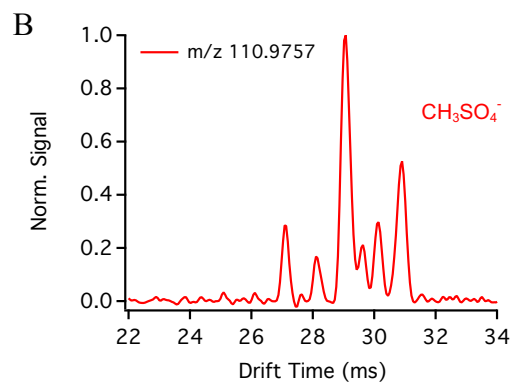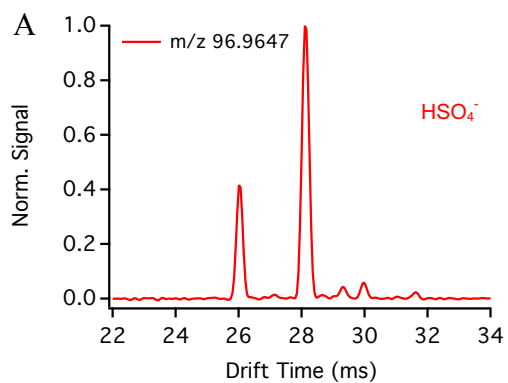
Figure 5 Organosulfate identification using IMS-TOF: A) Drift time of HSO$_4^-$ (m/z 96.9647); B) Drift time of CH$_3$SO$_4^-$ (m/z 110.9757); C) Drift time of CH$_3$SO$_4^-$ and m/z 297.0835 (assigned to C$_{10}$H$_{17}$O$_8$S$^-$). Overlapping of the drift times at 30.14 ms between the two mass-to-charge ratios indicates that the daughter ion CH$_3$SO$_4^-$ is a fragment ion of the parent ion C$_{10}$H$_{17}$O$_8$S$^-$.
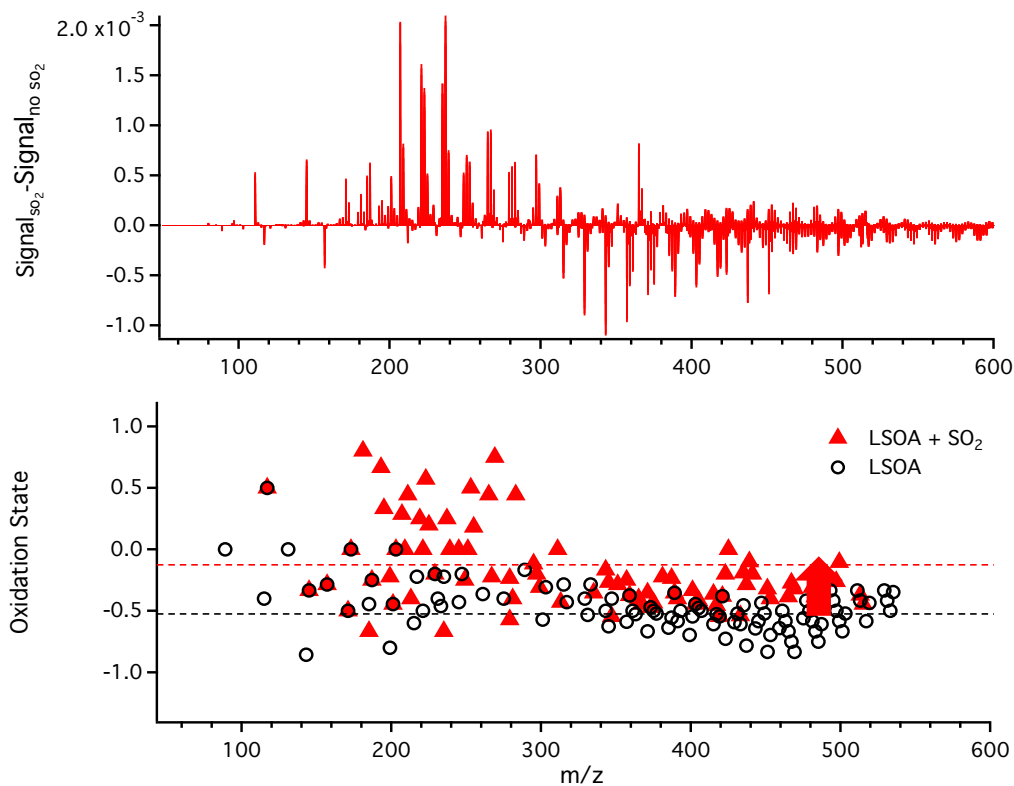
Figure 6 Difference of normalized mass spectra between LSOA in the presence and absence of SO$_2$ (top panel). Signal of HSO$_4^-$ (m/z 96.96) was excluded such that only organic mass spectra are compared. Bottom panel shows the average carbon oxidation state of each peak detected in IMS-TOF and the overall average carbon oxidation states of LSOA (black dashed line) and LSOA + SO$_2$ (red dashed line).
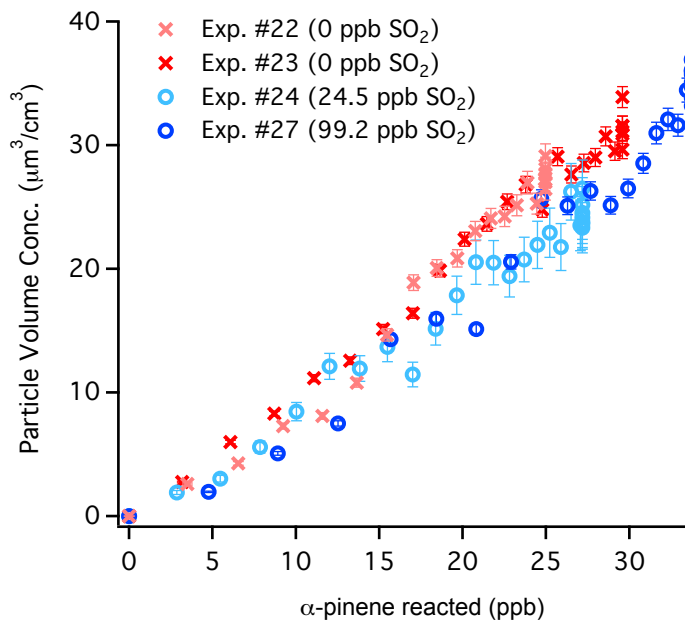
865 **Figure 7** Growth of particle volume concentration as a function of reacted α-pinene under dry conditions. No significant change of SOA formation was observed.
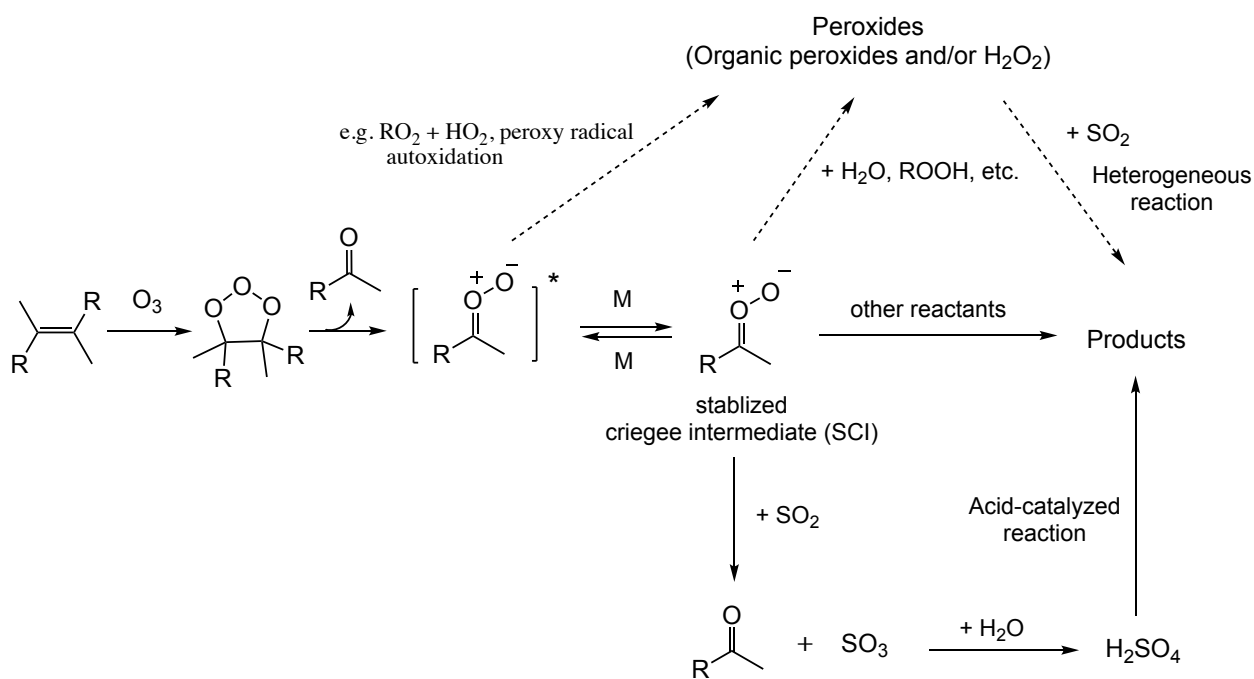
870

Scheme 2 The proposed reaction mechanisms for SO_2 and reactive intermediates in monoterpene ozonolysis.
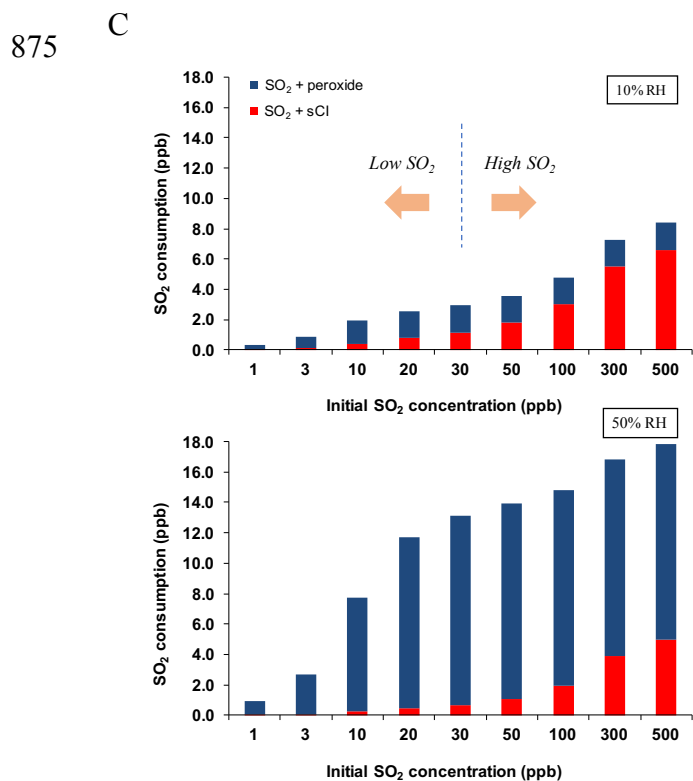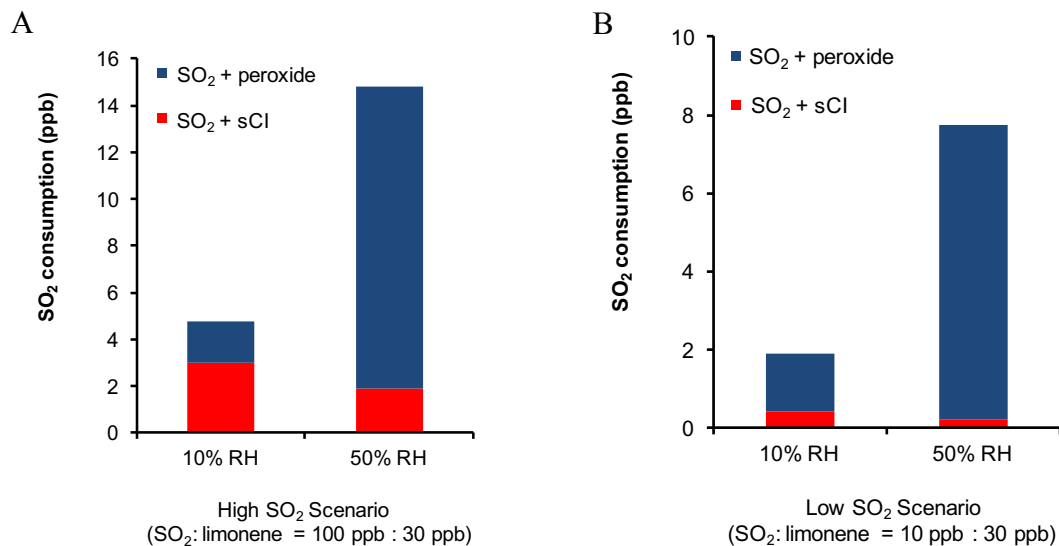
Figure 8 SO$_2$ consumption through reactions with sCI and peroxide under different humidity conditions in a high SO$_2$ scenario (100 ppb, panel A) and a low SO$_2$ scenario (10 ppb, panel B). And SO$_2$ consumption as a function of initial SO$_2$ concentration under different humidity conditions (panel C).

875

880